Structure and Dynamics of the Myristoyl Lipid Modification of Src Peptides Determined by ^{2}H Solid-State NMR Spectroscopy

Holger A. Scheidt[†‡] and Daniel Huster[†*]

[†]Institute of Medical Physics and Biophysics, University of Leipzig, 04107 Leipzig, Germany; and [‡]Structural Biology of Membrane Proteins Junior Research Group, Institute of Biochemistry/Biotechnology, Martin Luther University Halle-Wittenberg, 06120 Halle/Saale, Germany

ABSTRACT Lipid modifications of proteins are widespread in nature and play an important role in numerous biological processes. The nonreceptor tyrosine kinase Src is equipped with an N-terminal myristoyl chain and a cluster of basic amino acids for the stable membrane association of the protein. We used ^{2}H NMR spectroscopy to investigate the structure and dynamics of the myristoyl chain of myr-Src(2–19), and compare them with the hydrocarbon chains of the surrounding phospholipids in bilayers of varying surface potentials and chain lengths. The myristoyl chain of Src was well inserted in all bilayers investigated. In zwitterionic 1,2-dimyristoyl-*sn*-glycero-3-phosphocholine membranes, the myristoyl chain of Src was significantly longer and appears "stiffer" than the phospholipid chains. This can be explained by an equilibrium between the attraction attributable to the insertion of the myristoyl chain and the Born repulsion. In a 1,2-dimyristoyl-*sn*-glycero-3-phosphocholine/1,2-dimyristoyl-*sn*-glycero-3-[phospho-*L*-serine] membrane, where attractive electrostatic interactions come into play, the differences between the peptide and the phospholipid chain lengths were attenuated, and the molecular dynamics of all lipid chains were similar. In a much thicker 1,2-dipalmitoyl-*sn*-glycero-3-phosphocholine/1,2-dipalmitoyl-*sn*-glycero-3-[phospho-*L*-serine]/cholesterol membrane, the length of the myristoyl chain of Src was elongated nearly to its maximum, and the order parameters of the Src chain were comparable to those of the surrounding membrane.

INTRODUCTION

About one third of the human genome encodes for membrane proteins (1,2), which are essential for many important cellular processes such as signal transduction or membrane transport. In particular, for biological processes that are mediated by protein-protein interactions such as biological signal transduction, membrane binding drastically increases the probability of intermolecular contacts, because the diffusion of proteins at the membrane surface is restricted to two dimensions. In addition to internal membrane proteins that feature transmembrane α-helices or β-barrels, nature has evolved peripheral membrane proteins that bind to the membrane surface by glycosylphosphatidylinisotol (GPI) anchors or covalently attached lipid modifications. The latter are particularly common for proteins involved in signal transduction (3), and comprise an astonishing structural variety, including myristoyl or palmitoyl lipid chains, farnesyl or geranylgeranyl modifications, or covalently attached cholesterol (4). These motifs attach the proteins to cellular membranes via hydrophobic interactions, often combined with electrostatic contributions (3,5). Consequently, the biophysics of such membrane binding is characterized by a very complex interplay of different physical interactions. Although lipid-modified proteins are widespread in nature and perhaps membrane anchoring is not their only function (roles in protein-protein interaction, protein activation, and protein stabilization were also discussed) (6–8), only little structural information is available about these proteins.

A combination of lipid chain insertion and electrostatic attraction is relevant for the membrane binding of a number of peripheral membrane proteins (e.g., Src, MARCKS, HIV-1 Gag, and K-Ras4B). In particular, for Src (a membrane-bound nonreceptor tyrosine kinase from the *Rous sarcoma* virus) (9), a number of interesting biological and biophysical findings have promoted an understanding of the molecule's biological function. Most importantly, nonmyristoylated mutants of the Src protein did not induce morphological transformations of infected cells, although wild-type levels of the phosphorylation of cellular proteins on tyrosine were evident in these cells (10,11). Detailed studies of the biophysics of the membrane-binding mechanism of N-terminal peptides from Src (12) revealed that the molecule comprises two distinct features that are involved in membrane binding. Next to the myristoylated N-terminal glycine, a cluster of basic amino acids is found in the peptide sequence, i.e., at position 5, 7, 9, and 13–15. Consequently, binding to membranes that contain increasing fractions of acidic phospholipids is largely enhanced (12). Further, the standard Gibbs free energy for binding for simple myristoylated peptides, as well as for myristoylated Src to zwitterionic membranes, was determined to be around −8 kcal/mol (13). Based on partitioning experiments with free fatty acids and lipidated peptides, it was shown that each membrane-inserted methylene group constitutes about −0.8 kcal/mol free energy (13–15). Consequently, Murray et al. (5) and Buser et al. (12) concluded that only about 10 methylene groups of the myristoyl chain are inserted into the membrane, whereas the rest of the chain is localized in the membrane headgroup region. This structural

Submitted November 28, 2008, and accepted for publication February 17, 2009.

*Correspondence: daniel.huster@medizin.uni-leipzig.de

Editor: Marc Baldus.

0006-3495/09/05/3663/10 $2.00

doi: 10.1016/j.bpj.2009.02.028

arrangement is the result of the balance between attractive coulombic and hydrophobic interactions and the Born repulsion (5). However, this interesting scenario, as based on thermodynamic considerations, has never been tested by structural methods. Here, we used quantitative ^{2}H NMR measurements to determine the geometry of the myristoyl chain of Src peptides, to provide a structural basis for these findings.

Static ^{2}H solid-state NMR is an excellent tool for studying the structure and dynamics of lipid modifications of proteins and peptides (16–21). Deuteration of hydrocarbon chains allows a determination of segmental order fluctuations, corresponding to the amplitudes of segmental motions in the membrane. Further, the elasticity and deformations of lipid membranes, and detailed geometric parameters of hydrocarbon chains, can be elucidated via ^{2}H NMR data (16,22,23). Switching the deuterium label between lipid chains of the membrane and peptide ^{2}H solid-state NMR also allows for investigations of the structure and dynamics of the host membrane. In particular, the comparison of properties of the lipid matrix with those of lipid modifications of the respective protein offers important insights into the biophysics of the membrane-binding mechanism (16).

We present an investigation of an N-terminal Src peptide (amino acids 2–19) bound to phospholipid membranes of varying surface potentials and hydrocarbon chain lengths. The Src peptide has a net charge of +4 at physiological pH, and a 14-carbon myristoyl chain attached to the N-terminal glycine. Since only three amino acids of the peptide have a hydrophobic character, there should be no significant contribution to the Gibbs free energy for binding of the peptide. We compare the properties of the myristoyl chain of this peptide and the hydrocarbon chains of the host membrane, with a different composition to study the influence of membrane charge and thickness.

MATERIALS AND METHODS

Materials

The phospholipids 1,2-dimyristoyl-*sn*-glycero-3-phosphocholine (DMPC), 1,2-dimyristoyl-*sn*-glycero-3-[phospho-*L*-serine] (DMPS), 1,2-dipalmitoyl-*sn*-glycero-3-phosphocholine (DPPC), 1,2-dipalmitoyl-*sn*-glycero-3-[phospho-*L*-serine] (DPPS), and the analogs of these molecules with perdeuterated acyl chains (DMPC-d_{54}, DMPS-d_{54}, DPPC-d_{62}, and DPPS-d_{62}), as well as cholesterol, were purchased from Avanti Polar Lipids (Alabaster, AL), and were used without further purification.

The myristoylated Src peptides (representing amino acids 2–19 of the Src protein) with the sequence myr-GSSKSKPKD PSQRRRSLE were synthesized using a standard Fmoc peptide synthesis protocol. Either the Src peptide with a protonated (myr-Src) or a perdeuterated myristoyl chain (myr-d_{27}-Src) was synthesized. Deuterated myristic acid was purchased from Euriso-Top (Saarbrücken, Germany).

Sample preparations

The lipids and their mixtures were prepared in chloroform or chloroform/methanol solution at the desired mixing ratios. After evaporating the solvent, the lipid film was resuspended in buffer solution (50 mM HEPES and 10 mM NaCl, pH 7.4). From this suspension, large unilamellar vesicles (LUVs) were prepared by extrusion, according to standard procedures (24). Aliquots of the Src peptide were added to the LUV preparations at a molar peptide/lipid ratio of 1:20, and incubated overnight. During incubation, several freeze-thaw cycles were applied, to enable binding of the peptide to the inner leaflet of the membrane. All preparation steps were conducted at temperatures above the phase-transition temperature of the lipids. After incubation, the suspension was ultracentrifuged for 1.5 h at 79,000 × *g*. The pellet was lyophilized overnight, rehydrated with 35 wt % deuterium-depleted water, and transferred into 5-mm glass vials and tightly sealed for NMR measurements. To determine the protein concentration of the supernatant, a standard bicinchoninic acid (BCA) protein test (Sigma-Aldrich, Deisenhofen, Germany) was used.

^{2}H NMR measurements

The ^{2}H NMR spectra were acquired on a Bruker Avance 750 MHz NMR spectrometer (Bruker Biospin, GmbH, Rheinstetten, Germany), operating at a resonance frequency of 115.1 MHz for ^{2}H. A single-channel solids probe equipped with a 5-mm solenoid coil was used. The ^{2}H NMR spectra were accumulated with a spectral width of ±250 kHz, using quadrature phase detection. A phase-cycled quadrupolar echo sequence (25) was used. The typical length of a 90° pulse was 2.7–3.0 μs, and a relaxation delay of 2 s was applied. For measurement of T_1 spin-lattice relaxation times, a phase-cycled inversion-recovery quadrupolar echo pulse sequence, with 11 time delays between 1 ms and 2.5 s and a relaxation delay of 2.5 s, was used. All measurements were conducted at a temperature of 303 K.

The ^{2}H NMR powder spectra were dePaked (26) using the algorithm of McCabe and Wassall (27), and the order parameter profiles of acyl chains were determined by a numerical spectral fitting procedure, based on the observed quadrupolar splitting $\Delta\nu_Q(n)$:

$$\Delta\nu_Q(n) = \frac{3}{4}\frac{e^2qQ}{h}S(n), \quad (1)$$

where e^2qQ/h is the quadrupole coupling constant (167 kHz for ^{2}H in a C-^{2}H bond), and $S(n)$ is the chain order parameter for the nth carbon position in the chain. The length of the acyl chain L_c* (''chain extent'') and the mean interfacial area (A) were calculated according to the mean torque model (16,22).

For analysis of relaxation measurements, the line shape of the ^{2}H NMR powder spectra with the longest delay time was simulated by a superposition of the respective number of Pake doublets, using Mathcad 2001 (MathSoft Engineering and Education, Cambridge, MA). The program determines the relaxation time for each individual Pake doublet by a fitting procedure that calculates the ^{2}H NMR spectrum for each inversion recovery delay, and compares it with the experimental spectrum.

^{31}P NMR measurements

Static ^{31}P NMR spectra were measured on a Bruker DRX 600 NMR spectrometer operating at a resonance frequency of 242.8 MHz for ^{31}P, using a Hahn echo pulse sequence. A ^{31}P 90° pulse length of 11 μs, a Hahn echo delay of 50 μs, a spectral width of 100 kHz, and a recycle delay of 2.5 s were used. Continuous-wave low-power proton decoupling was applied during signal acquisition. The measured NMR spectra were simulated using a program written in Mathcad 2001 to obtain the chemical-shift anisotropy.

RESULTS

Peptide binding

Before the NMR experiments, the amount of Src peptide bound to LUVs was determined in a centrifugation assay.

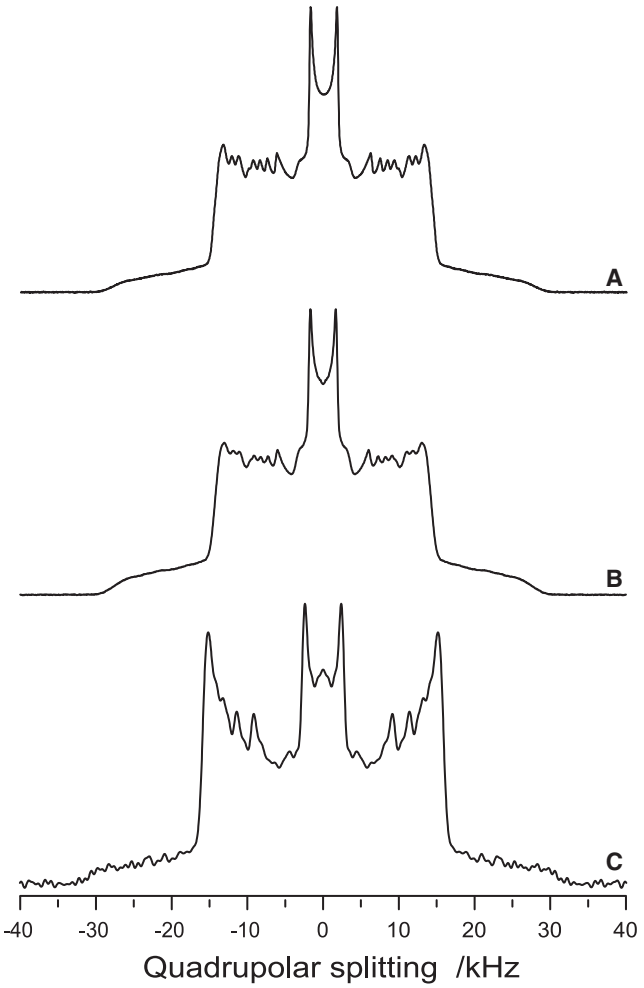

FIGURE 1 The 115.1 MHz solid-state ^{2}H NMR spectra of (*A*) pure DMPC-d_{54}, (*B*) DMPC-d_{54}/myr-Src, and (*C*) DMPC/myr-d_{27}-Src at temperature of 303 K. The peptide/lipid molar ratio was <1:20.

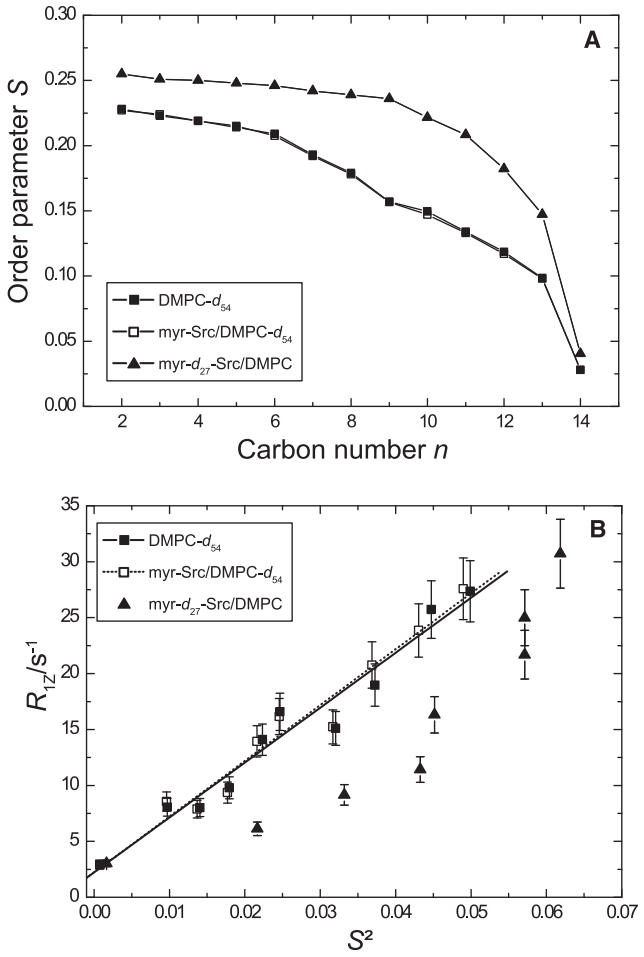

FIGURE 2 (*A*) ^{2}H NMR order parameter plot for the DMPC acyl chains in the presence (*open symbols*) and absence (*solid symbols*) of myr-Src and the deuterated myristoyl chain of myr-d_{27}-Src (▲) at 303 K. (*B*) Dependence of spin-lattice relaxation rate R_{1Z} on the square of the corresponding segmental order parameter S^2 for DMPC membranes in the presence and absence of Src, and for the Src myristoyl chain. Same symbols were used as in *A*. Lines represent linear regressions for the phospholipid chains. The peptide/lipid molar ratio was <1:20.

This analysis revealed that about 50% of the Src peptide was bound to the zwitterionic DMPC vesicles. For membranes composed of phosphatidylcholine (PC) and phosphatidylserine (PS), the amount of bound peptide increased to >80%, confirming the importance of electrostatic interactions for the binding of Src peptides to phospholipid membranes (5,12,29). Therefore, the final peptide/lipid molar ratio of the final sample was <1:20.

Src lipid chain structure and dynamics in DMPC membranes

First, myr-Src was investigated in a simple zwitterionic DMPC membrane. The ^{2}H NMR spectra (Fig. 1) of DMPC-d_{54} in the absence and presence of myr-Src, as well as of the myristoyl chain of myr-d_{27}-Src in a protonated DMPC matrix, showed the typical powder spectrum characteristics of a lamellar liquid-crystalline lipid membrane with a superposition of the Pake doublets of the different methylene and methyl groups. Interestingly, the spectrum of the myristoyl chain of myr-d_{27}-Src (Fig. 1 *C*) clearly exhibited larger quadrupolar splittings than did the spectrum of the surrounding DMPC membrane (Fig. 1 *B*). In this spectrum, a small isotropic peak was detected that may be attributable to highly mobile Src peptide or residual HDO. A quantitative analysis of this isotropic peak revealed that it contributes much <5%, indicating that at maximum, 5% of the Src peptide may not be associated with the membrane presumably forming micelles.

Based on these ^{2}H NMR spectra, order parameter profiles can be calculated, as shown in Fig. 2 *A*. The order parameter plots for DMPC-d_{54} in the presence and absence of myr-Src are virtually identical, indicating that peptide binding does not influence the structure and dynamics of the lipid matrix (the typical error for the order parameter determination is smaller than the symbol size in Fig. 2 *A*). Consequentially, the calculated geometric parameters of the hydrocarbon

TABLE 1 Calculated geometric parameters of phospholipid and Src lipid chains: mean interfacial areas of one chain (*A*) and chain extent (L_c*) for deuterated hydrocarbon chains in all investigated samples

	A/Å^2	L_c*/Å
DMPC-d_{54}	29.2	10.3
myr-Src/DMPC-d_{54}	29.2	10.2
myr-d_{27}-Src/DMPC	27.9	11.5
DMPC-d_{54}/DMPS	27.6	10.7
DMPC/DMPS-d_{54}	27.7	10.7
myr-Src/DMPC-d_{54}/DMPS	28.8	10.3
myr-Src/DMPC/DMPS-d_{54}	28.2	10.7
myr-d_{27}-Src/DMPC/DMPS	27.8	11.3
DPPC-d_{62}/DPPS/cholesterol	22.4	15.7
DPPC/DPPS-d_{62}/cholesterol	22.3	15.7
myr-Src/DPPC-d_{62}/DPPS/cholesterol	22.6	15.2
myr-Src/DPPC/DPPS-d_{62}/cholesterol	22.5	15.4
myr-d_{27}- Src/DPPC/DPPS/cholesterol	22.4	14.1

chain, such as mean interfacial area A and the chain extent L_c*, are nearly identical (Table 1). These results can be confirmed in the measured static ^{31}P NMR spectra (not shown), which exhibit the typical line shape for a lamellar liquid-crystalline phase. In these spectra, the same chemical-shift anisotropy for the phosphate group of DMPC in the absence and presence of myr-Src was measured, and indicated no influence of peptide binding on lipid headgroup flexibility.

However, a much different picture was obtained for the myristoyl chain of myr-d_{27}-Src. The ^{2}H NMR order parameters were significantly increased for the entire lipid chain (Fig. 2 *A*). Although the Src lipid chain contains the same number of carbons as DMPC, its length L_c* was increased by 1.3 Å, meaning that the hydrocarbon chain of the peptide is more extended than the chains of the surrounding phospholipids. Correspondingly, the interfacial area of one chain A was decreased (Table 1). This means that the Src peptide exhibits the opposite behavior compared with other lipidated proteins such as Ras and GCAP-2, where the length of the lipid modification is nearly perfectly adapted to the length of the surrounding lipid membrane (16,21).

To study the dynamics of hydrocarbon chains, ^{2}H NMR longitudinal relaxation rates R_{1Z} were measured. The relaxation process is determined by random fluctuations of electromagnetic fields attributable to internal motions (23). Although a comprehensive set of experimental data (i.e., field dependence, angular-dependent relaxation rates of oriented membranes, or various relaxation rates such as Zeeman or quadrupolar order) can provide detailed quantitative insights into motional processes (21,30–32), we focused on a qualitative description of lipid-chain mobility. To this end, the correlation of Zeeman order relaxation rate R_{1Z} with the square of the segmental order parameter S^2 proved to be a useful qualitative tool (23,33). For pure saturated phospholipid membranes, these plots exhibit a linear dependence with a specific positive slope (23). Changes in the dynamics of lipid chains alter these square law plots. For instance, the addition of cholesterol to saturated membranes increases the lipid chain order by decreasing the amplitude of order fluctuations. In the square law plot, this is expressed by a shallower slope of the linear curve. In contrast, soft membranes that are characterized by larger amplitude fluctuations (e.g., mixtures of saturated phospholipids and detergents) exhibit square law plots with a steeper slope, and usually provide a characteristic curved shape (16,34,35).

The square law plots obtained for the Src peptide and surrounding DMPC matrix are shown in Fig. 2 *B*. As anticipated, the plots for DMPC-d_{54} in the absence and presence of myr-Src are nearly identical, and exhibit the expected linear behavior. The myristoyl chain of myr-d_{27}-Src in a DMPC matrix does not really exhibit a linear square law plot, but the slope of the curve is decreased compared with DMPC. This indicates the lower mobility of the more elongated hydrocarbon chain of the Src peptide.

It is tempting to argue that the square law plot of the Src lipid modification follows a quadratic rather than a linear behavior, although such square law plots have not been reported, to the best of our knowledge. Certainly, the structural and dynamic properties of Src myristoyl lipid modification in the DMPC membrane are also unique, and the physical background of this interesting behavior calls for further exploration.

Src lipid chain structure and dynamics in DMPC/DMPS membranes

To study the influence of surface potential of the membrane on the structure and dynamics of the lipid chain of the Src peptide, a lipid matrix composed of the zwitterionic DMPC and negatively charged DMPS (molar ratio, 7:3) was investigated. A fraction of 30% negatively charged lipids also mimics the situation on the inner leaflet of eukaryotic plasma membranes quite well, to which the Src protein is bound. For ^{2}H NMR measurements, either one of the phospholipid species or the Src peptide was labeled with a perdeuterated 14:0 lipid chain.

The calculated order parameter plots for DMPC-d_{54} or DMPS-d_{54} in the absence of myr-Src exhibit only marginal differences (Fig. 3 *A*), indicating a homogeneous mixture of lipids in the membrane. When myr-Src is added, a decrease in the order parameter in the upper chain region is observed for both lipids, whereas in the lower chain region, the plots are very similar to the order profiles in the absence of myr-Src. This provides an indication of the distortion of the membrane because of peptide binding. Surprisingly, the decrease is more pronounced for the zwitterionic DMPC-d_{54} than for DMPS-d_{54}.

Although this difference in order between the two lipid species is rather small, it could be an indication of peptide-induced phase separation or lipid demixing, as observed in other peptides such as MARCKS (36,37), P828 (38), phospholamban (39), or polylysine (40).

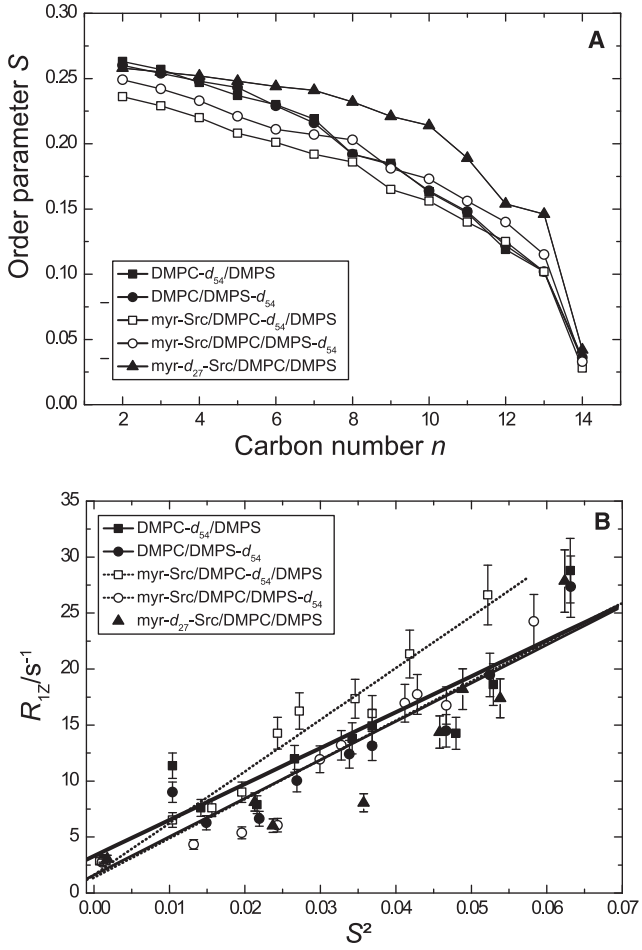

FIGURE 3 (*A*) ^{2}H NMR order parameter plot for acyl chains of DMPC/DMPS mixtures (7:3) in the presence (*open symbols*) and absence (*solid symbols*) of myr-Src and the deuterated myristoyl chain of myr-d_{27}-Src (▲) at 303 K. (*B*) Dependence of R_{1Z} rates on the corresponding squared order parameter S^2 for the phospholipid acyl chains in the presence and absence of myr-Src and the deuterated myristoyl chain of myr-d_{27}-Src. Same symbols were used as in *A*. Lines represent linear regressions for the phospholipid chains. Measurements were performed at a molar peptide/lipid ratio of <1:20.

The differences in chain order between lipid species are also illustrated by the geometric parameters of the acyl chains given in Table 1. Only the chains of DMPC-d_{54} of the mixture show slightly reduced chain length in the presence of myr-Src. Moreover, in the static ^{31}P NMR spectra (not shown), a decrease in the chemical shift anisotropy of about 2 ppm for DMPC and DMPS in the presence of myr-Src reveals this influence of peptide binding on headgroup flexibility and therefore on membrane organization.

For the myristoyl chain of myr-d_{27}-Src in DMPC/DMPS, the order parameters are again somewhat larger than for the surrounding phospholipid molecules, but the difference is not as pronounced as for a pure DMPC membrane. The higher order parameters are mostly encountered in the middle and lower chain regions. For the upper chain, they are quite similar to those of the membrane in the absence of myr-Src. In quantitative numbers, the myristoyl chain length L_c* for myr-d_{27}-Src is 0.6 Å longer than the chains of DMPS in the mixture, and 1.0 Å longer than the chains of DMPC.

In square law plots (Fig. 3 *B*), similar behavior is evident. Considering the error bars on the data points, it is fair to say that these plots are comparable for all lipids in the presence and absence of myr-Src. Only for myr-Src/DMPC-d_{54}/DMPS was a slightly steeper slope observed, indicating higher mobility, as already suggested by the decreased order parameters. This finding suggests more similar dynamics of the lipid and peptide hydrocarbon chains in a DMPC/DMPS matrix than in the zwitterionic DMPC membrane. The square law plot of the myristoyl chain of the Src peptide is closer to the phospholipid plots than in the pure DMPC matrix. However, a deviation from a perfectly linear behavior is again evident.

Src lipid chain structure and dynamics in DPPC/DPPS/cholesterol membranes

To study the structure and dynamics of the lipid modification of myr-Src in a lipid membrane with a hydrocarbon core that is much thicker than the length of the myristoyl chain of myr-Src, a DPPC/DPPS/cholesterol (molar ratio, 7:3:10) matrix was investigated. This lipid mixture represents the liquid ordered (l_o) phase, as observed in lipid rafts. With a cholesterol content of 50 mol %, there will be no phase transition or gel phase (41). The palmitoyl chains of these disaturated phospholipids are two methylene groups longer then the myristoyl chain of the peptide. In addition, the acyl chains are elongated because of the lipid condensation effect of cholesterol, which leads to condensation and the formation of the l_o phase. This phase is characterized by a tighter packing of the lipid molecules, decreased lateral diffusion, and an increase in phospholipid chain order parameters and therefore of chain length (42–46).

The ^{2}H NMR spectra of the phospholipids of the mixture, as well as that of the myristoyl chain (Fig. 4), are significantly broader than those in the absence of cholesterol. The NMR spectra show the typical signature of lipids in the l_o phase (47–51). The ^{2}H NMR spectra of phospholipids in the mixture give indications of domain formation, as seen in the additional set of quadrupolar splittings observed for the terminal methyl group signal (47). A characteristic feature of the ^{2}H NMR spectrum of the myristoyl chain of Src is the significantly larger quadrupolar splitting of $\Delta\nu_Q \approx 40$ kHz for the methylene group next to the methyl group of the chain end for the myristoyl chain of myr-d_{27}-Src (Fig. 4 *E*), compared with the phospholipid chains.

The ordering effect of cholesterol is also evident in the order parameter plots for the lipid mixture (Fig. 5). In all plots, largely increased order parameters, compared with the previous samples, are evident. Again, the plots in the

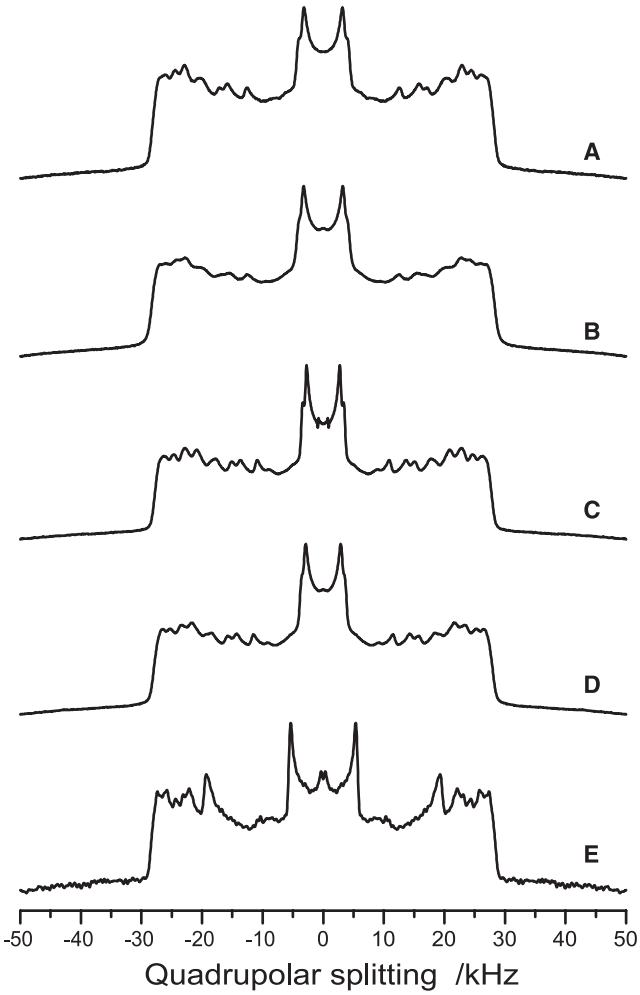

FIGURE 4 The 115.1 MHz solid-state ^{2}H NMR spectra for (*A*) DPPC-d_{62}/DPPS/cholesterol, (*B*) DPPC/DPPS-d_{62}/cholesterol, (*C*) myr-Src/DPPC-d_{62}/DPPS/cholesterol, (*D*) myr-Src/DPPC/DPPS-d_{62}/cholesterol, and (*E*) myr-d_{27}-Src/DPPC/DPPS/cholesterol at 303 K.

absence of myr-Src are similar for DPPC-d_{62} and DPPS-d_{62}, demonstrating the relatively good miscibility of these phospholipids and cholesterol, even at this high cholesterol concentration. In the presence of myr-Src, the order parameters of the two phospholipids are somewhat decreased but still quite similar, which indicates minor disturbances in the membrane organization because of the binding of the peptide, as already observed for the DMPC/DMPS matrix. Again, the small differences in order in the presence of the Src peptide could indicate nonideal mixing of the two components of the mixture.

The conclusions based on an inspection of the order parameter plots are mirrored in the geometric parameters for the hydrocarbon chains in Table 1. For myr-d_{27}-Src bound to the DPPC/DPPS/cholesterol membrane, the ^{2}H NMR chain order parameters are now quite similar to that of the phospholipid. Only a slight increase in the middle chain region is visible.

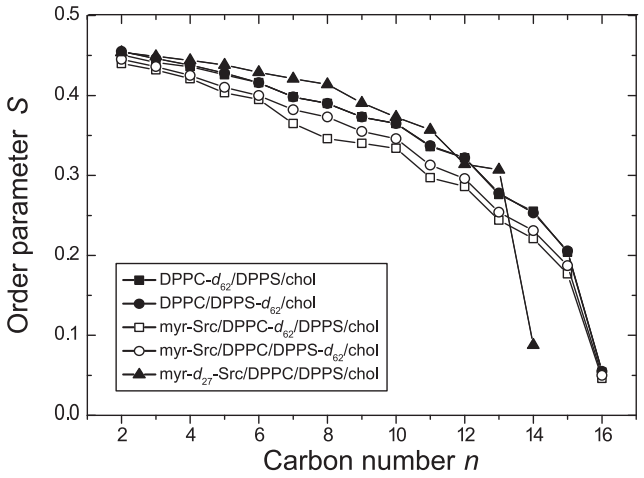

FIGURE 5 ^{2}H NMR order parameter plot for the acyl chains of DPPC/DPPS/cholesterol mixtures (7:3:10) in the presence (*open symbols*) and absence (*solid symbols*) of myr-Src and the deuterated myristoyl chain of myr-d_{27}-Src (▲).

DISCUSSION

Despite the widespread occurrence of lipid-modified proteins in nature, only a little structural and dynamic information about these membrane-bound molecules is available (4,19,21). Lipid modifications in proteins may fulfill different tasks. The most straightforward function involves the membrane anchor that provides soluble proteins with sufficient hydrophobic energy to associate with the membrane. This function can be triggered to distinguish between the cytosolic and membrane-associated states of a protein (6). Further, lipid modifications are thought to play a role in protein-protein interactions and protein activation (8), and in the stabilization of protein structures (7). Perhaps the best studied system is human Ras, where chemical biology approaches allowed a synthesis of fully functional lipidated Ras molecules with the respective lipid modifications (4,52–54). Both experimental and computational methods aided in the understanding of the membrane binding of Ras (55,56). In particular, ^{2}H NMR is a method well suited to studying the structure and dynamics of lipid-chain modifications of lipidated Ras and other proteins with covalently attached lipid chains (17).

The ^{2}H NMR data of this study clearly show that the myristoyl group of Src is inserted in the membrane. This represents the major binding mechanism of those peptides. Our binding measurements confirmed that ~50% of the Src peptide binds to zwitterionic membranes, which corresponds to a ΔG for partitioning from the aqueous phase to the membrane of approximately −35 kJ/mol. This value is relatively close to the value of −30 kJ/mol for the partitioning of a free myristic acid into *n*-heptane (14). Our results also agree well with the precise measurement of myristoylated peptide partitioning into lipid membranes that revealed a unitary Gibbs free energy of approximately −33.5 kJ/mol

(13). As discussed by Murray et al. (5), electrostatic interactions can enhance the binding of myristoylated peptides. In our preparation, the 30 mol % PS in the membrane increased the Gibbs free energy to approximately −39 kJ/mol, which means that more than 80% of the peptide is bound to the membrane. Therefore, to provide stable binding of Src to phospholipid membranes, both the hydrophobic interaction of the N-terminal myristoyl chain and the electrostatic interactions of the charged amino acids are necessary (12,29).

In this study, we investigated the structure and dynamics of the myristoyl chain of myr-Src(2–19), compared with the hydrocarbon chains of the surrounding phospholipid molecules. It was previously suggested that less than the entire myristoyl chain of Src peptides is inserted into membranes, and that the remaining carbons are located in the membrane headgroup region, whereas the polar N-terminal glycine remains outside the bilayer, just above the lipid headgroups (5,12,29). This would be caused by the complex interplay of different physical interactions between the peptide and the lipid membrane. The position of the peptide is determined by the minimal free energy balanced between the attractive long-range hydrophobic and electrostatic forces between the clusters of basic amino acids of myr-Src and the lipid headgroups, and the short-range Born repulsion. Born repulsion arises from the image charge that repels the peptide from a low dielectric membrane surface. There are also weaker attractive electrostatic interactions with zwitterionic membranes, because the lipid headgroups represent permanent electric dipoles. Moreover, entropic contributions to the Gibbs free energy must be considered, because the entropic losses attributable to the binding of a lipid-modified peptide to the membrane can already compensate for the energy gained because of the insertion of a hydrocarbon chain into the membrane (37).

Our ^{2}H NMR measurements allow for a precise determination of the length of the peptide's myristoyl chain, compared with the chains of the surrounding phospholipids in the membrane. Fig. 6 provides a visual summary of this study's experimental findings. The ^{2}H NMR measurements confirm that the myristoyl chain of Src is longer than the surrounding phospholipid chains, as suggested by Murray et al. (5). Such a situation is new in the literature, and contrary to what is known for Ras and guanylate cyclase-activating protein (GCAP), where lipid modifications adapt to the length of the surrounding membrane (16,21). Interestingly, the largest chain mismatch is observed in zwitterionic DMPC membranes. Here, the Src myristoyl chain is ~1.3 Å longer than the DMPC chains. This corresponds approximately to the length alteration induced by one fewer *gauche* defect, which typically reduces an acyl chain by 1.1 Å (57). Of course, this chain conformation is not static. Rather, the situation is brought about by the molecular dynamics of the myristoyl chain with frequent *trans-gauche* isomerizations, as conveyed by the ^{2}H order parameters. Because the Src chain is longer than the myristoyl chain of the surrounding lipids, it appears ''stiffer'' than the surrounding DMPC chains in the square law plots that provide a measure of the elasticity and molecular dynamics of the membrane.

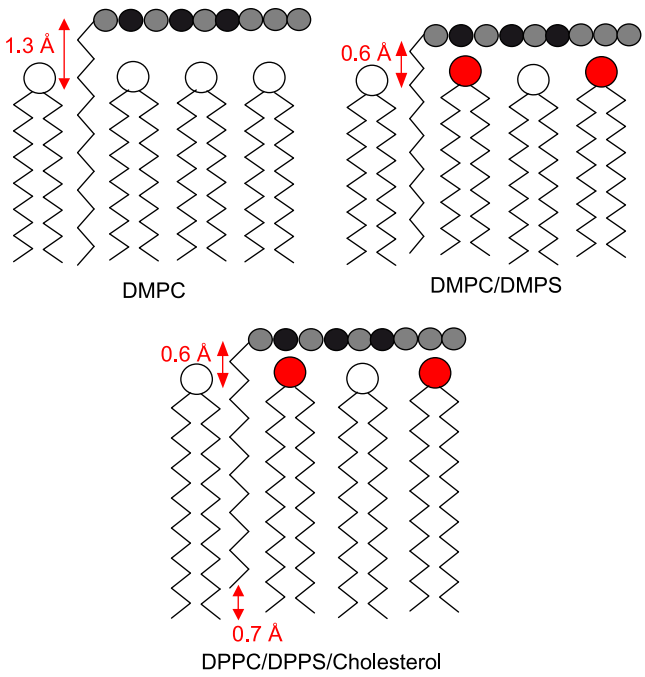

FIGURE 6 Schematic representation of the membrane position of the Src peptide and length of the hydrocarbon chain in different lipid matrices. Arrows indicate the chain-length mismatch between the Src myristoyl chain and the acyl chains of the host membrane. Acidic phospholipid headgroups are highlighted. Basic amino acids are shown in black.

Zwitterionic membranes can add only a small contribution to attractive electrostatic forces. When negatively charged phospholipids are included in the lipid matrix, the binding of Src peptides increased noticeably (12,29). Our ^{2}H NMR measurements revealed that in a DMPC/DMPS membrane, the differences in peptide versus phospholipid chain lengths is attenuated to ~0.6–1 Å. Further, the molecular dynamics of all chains, i.e., phospholipid and peptide, are more similar. Because of the increased attractive electrostatic interactions between the membrane and the peptide, the free energy minimum is shifted, and the myristoylated N-terminus of the peptide inserts deeper into the headgroup region of the membrane. This, in turn, may disturb lipid-membrane organization, which explains the small decrease in the order parameters of phospholipids and in the chemical-shift anisotropy in ^{31}P NMR spectra in the presence of myr-Src.

The thermodynamic measurements by Buser et al. (12) suggested that only ~10 methylene groups of the myristoyl moiety of the Src peptide inserted into the membrane. Our ^{2}H NMR chain-length difference between the Src myristoyl chain and the chains of the surrounding membrane can only account for about one CH_2 group, which would not be inserted into the membrane. However, neither NMR nor thermodynamic measurements can reveal whether the terminal

methyl groups of the chain are localized at the same *z* coordinate in the membrane center. For optimal membrane packing, one would assume that the myristoyl chain has to be elongated, to reach down into the hydrophobic membrane core. However, an incomplete insertion of the Src chain may also be possible, albeit energetically more costly. This energy penalty, however, would be traded for the attenuated Born repulsion of a polar peptide backbone that is localized more distantly from the membrane surface.

For a better understanding of this issue, we studied an extreme case: the partitioning of the myr-Src peptide into DPPC/DPPS membranes in the presence of 50 mol % cholesterol. Because of cholesterol-induced condensation, the phospholipid chains are even longer than the two extra methylene groups in each chain. Further, the lipids are found in the liquid-ordered phase state, and the phase transition is abolished. Although the liquid-ordered phase state of the membrane represents the biological raft phase, the DPPC/DPPS/cholesterol mixture used here was more physicochemically than biologically motivated. It was intended only to prepare a membrane with very long, elongated lipid chains, to see how the Src peptide would adapt its length to this hydrophobic thickness. In this situation, the molecular dynamics of the lipid chains were again altered to provide an adaptation to the alleged chain-length mismatch. First, the phospholipid chains increased their motional amplitudes, resulting in a decrease of their length in the presence of Src peptide. This effect may even be more pronounced for phospholipids directly surrounding the Src peptide, but NMR only measures the ensemble average. Second, the chain length of myr-Src in the DPPC/DPPS/cholesterol membrane was almost 3 Å longer than in DMPC/DMPS membranes. However, the measured 14.1-Å length of the myristoyl chain of Src is still shorter than the length of an all-*trans* 14:0 chain, which would be 15.2 Å. The all-*trans* chain would actually be closer to the length of the surrounding palmitoyl chains. However, the length difference that corresponds to just one *gauche* defect may represent a necessary entropic contribution to the free energy minimum of the entire ensemble. Third, the question remains as to whether the N-terminus of the peptide now inserts more deeply into the membrane, to allow for an alignment of the methyl groups of the chains, or if it remains at the same position as in the DMPC/DMPS membrane, and the positions of the methyl groups vary (Fig. 6).

It is also well known that cationic peptides can induce phase separation in mixed membranes (36–40). It was not within the scope of this study to investigate this issue systematically. Some indications for phase separation in membranes, such as pairs of quadrupolar splittings (47,50) and differences in quadrupolar splittings between lipid species (58), were evident. It remains to investigate this phenomenon further, particularly in membranes containing PIP_2, as it was shown to be highly relevant for the binding of MARCKS (59).

In conclusion, we studied the structure and dynamics of the lipid anchor of myristoylated Src. Because of the repulsive forces between the charged amino acids adjacent to the myristoylated N-terminus of the peptide and the membrane surface, the Src chain has higher order parameters than the surrounding lipid membrane composed of the same lipid chains. Even in a much thicker membrane, the order parameters of the Src chain are comparable to those of the surrounding membrane. This is in notable contrast to other lipidated proteins such as Ras, GCAP-2, or the surfactant protein SP-C, where the perfect adaptation of lipid modifications to the length of the surrounding membrane was observed (16,21,60). Because the full insertion of the Src myristoyl chain into the membrane would excessively increase the Born repulsion between charged peptide and low dielectric membrane, even the exposure of hydrophobic chain segments to the more hydrophilic headgroup region is tolerated, insofar as this structural arrangement provides the minimum in free energy. The length of the lipid-chain modification of a protein and its adaptation to the surrounding membrane is governed by the dynamics of the lipid chain. The amplitude of segmental motions in a protein's lipid chain is the decisive parameter that determines its adaptability to the surrounding membrane and membrane compartments. These biophysical results on the structure and dynamics of protein lipid chains, compared with these properties in the surrounding membrane, may aid in understanding why protein myristoylation might induce raft formation, or target lipidated proteins to preexisting rafts (61).

SUPPORTING MATERIAL

Nine equations are available at http://www.biophysj.org/biophysj/supplemental/S0006-3495(09)00586-4.

The authors are indebted to Prof. Stuart McLaughlin for helpful discussions. We thank the German Research Foundation (DFG) and the Experimental Physics Institutes of the University of Leipzig for providing measuring time on the Avance 750. The Src peptides were synthesized at the Interdisciplinary Center for Clinical Research Core Unit of the Medical Faculty at the University of Leipzig.

This study was supported by the Exzellenznetzwerk Biowissenschaften, funded by the state of Sachsen-Anhalt and the DFG (SFB 610).

REFERENCES

1. Yeagle, P. L., and D. A. Lee. 2002. Membrane protein structure. *Biochim. Biophys. Acta*. 1565:143.
2. Torres, J., T. J. Stevens, and M. Samso. 2003. Membrane proteins: the 'Wild West' of structural biology. *Trends Biochem. Sci.* 28:137–144.
3. Casey, P. J. 1995. Protein lipidation in cell signaling. *Science*. 268: 221–225.
4. Brunsveld, L., H. Waldmann, and D. Huster. 2009. Membrane binding of lipidated Ras peptides and proteins—the structural point of view. *Biochim. Biophys. Acta*. 1788:273–288.
5. Murray, D., N. Ben-Tal, B. Honig, and S. McLaughlin. 1997. Electrostatic interaction of myristoylated proteins with membranes: simple physics, complicated biology. *Structure*. 5:985–989.

6. Ames, J. B., R. Ishima, T. Tanaka, J. I. Gordon, L. Stryer, et al. 1997. Molecular mechanics of calcium-myristoyl switches. *Nature*. 389:198–202.
7. Haynes, L. P., and R. D. Burgoyne. 2008. Unexpected tails of a Ca^{2+} sensor. *Nat. Chem. Biol.* 4:90–91.
8. Hwang, J. Y., and K. W. Koch. 2002. Calcium- and myristoyl-dependent properties of guanylate cyclase-activating protein-1 and protein-2. *Biochemistry*. 41:13021–13028.
9. Resh, M. D. 1990. Membrane interactions of pp60v-src: a model for myristylated tyrosine protein kinases. *Oncogene*. 5:1437–1444.
10. Kamps, M. P., J. E. Buss, and B. M. Sefton. 1985. Mutation of NH_2-terminal glycine of p60src prevents both myristoylation and morphological transformation. *Proc. Natl. Acad. Sci. USA*. 82:4625–4628.
11. Cross, F. R., E. A. Garber, D. Pellman, and H. Hanafusa. 1984. A short sequence in the p60src N terminus is required for p60src myristylation and membrane association and for cell transformation. *Mol. Cell. Biol.* 4:1834–1842.
12. Buser, C. A., C. T. Sigal, M. D. Resh, and S. McLaughlin. 1994. Membrane binding of myristoylated peptides corresponding to the NH_2 terminus of Src. *Biochemistry*. 33:13093–13101.
13. Peitzsch, R. M., and S. McLaughlin. 1993. Binding of acylated peptides and fatty acids to phospholipid vesicles: pertinence to myristoylated proteins. *Biochemistry*. 32:10436–10443.
14. Tanford, C. 1980. The Hydrophobic Effect: Formation of Micelles and Biological Membranes. John Wiley & Sons, New York.
15. Pool, C. T., and T. E. Thompson. 1998. Chain length and temperature dependence of the reversible association of model acylated proteins with lipid bilayers. *Biochemistry*. 37:10246–10255.
16. Vogel, A., C. P. Katzka, H. Waldmann, K. Arnold, M. F. Brown, et al. 2005. Lipid modifications of a Ras peptide exhibit altered packing and mobility versus host membrane as detected by ^2H solid-state NMR. *J. Am. Chem. Soc.* 127:12263–12272.
17. Vogel, A., K. T. Tan, H. Waldmann, S. E. Feller, M. F. Brown, et al. 2007. Flexibility of Ras lipid modifications studied by ^2H solid-state NMR and molecular dynamics simulations. *Biophys. J.* 93:2697–2712.
18. Valentine, K. G., M. F. Mesleh, S. J. Opella, M. Ikura, and J. B. Ames. 2003. Structure, topology, and dynamics of myristoylated recoverin bound to phospholipid bilayers. *Biochemistry*. 42:6333–6340.
19. Koeppe, R. E., T. C. Vogt, D. V. Greathouse, J. A. Killian, and B. de Kruijff. 1996. Conformation of the acylation site of palmitoylgramicidin in lipid bilayers of dimyristoylphosphatidylcholine. *Biochemistry*. 35:3641–3648.
20. Reuther, G., K. T. Tan, A. Vogel, C. Nowak, K. Arnold, et al. 2006. The lipidated membrane anchor of full length N-Ras protein shows an extensive dynamics as revealed by solid-state NMR spectroscopy. *J. Am. Chem. Soc.* 128:13840–13846.
21. Vogel, A., T. Schroder, C. Lange, and D. Huster. 2007. Characterization of the myristoyl lipid modification of membrane-bound GCAP-2 by ^2H solid-state NMR spectroscopy. *Biochim. Biophys. Acta*. 1768:3171–3181.
22. Petrache, H. I., S. W. Dodd, and M. F. Brown. 2000. Area per lipid and acyl length distributions in fluid phosphatidylcholines determined by ^2H NMR spectroscopy. *Biophys. J.* 79:3172–3192.
23. Brown, M. F. 1982. Theory of spin-lattice relaxation in lipid bilayers and biological membranes. ^2H and ^{14}N quadrupolar relaxation. *J. Chem. Phys*. 77:1576–1599.
24. Mayer, L. D., M. J. Hope, and P. R. Cullis. 1986. Vesicles of variable sizes produced by a rapid extrusion procedure. *Biochim. Biophys. Acta*. 858:161–168.
25. Davis, J. H., K. R. Jefferey, M. Bloom, M. I. Valic, and T. P. Higgs. 1976. Quadropolar echo deuteron magnetic resonance spectroscopy in ordered hydrocarbon chains. *Chem. Phys. Lett*. 42:390–394.
26. Sternin, E., M. Bloom, and A. L. MacKay. 1983. De-Paking of NMR-spectra. *J. Magn. Reson.* 55:274–282.
27. McCabe, M. A., and S. R. Wassall. 1995. Fast Fourier transform dePaking. *J. Magn. Reson. B*. 106:80–82.
28. Reference deleted in proof.
29. Murray, D., L. Hermida-Matsumoto, C. A. Buser, J. Tsang, C. T. Sigal, et al. 1998. Electrostatics and the membrane association of Src: theory and experiment. *Biochemistry*. 37:2145–2159.
30. Bonmatin, J. M., I. C. P. Smith, H. C. Jarrell, and D. J. Siminovitch. 1990. Use of a comprehensive approach to molecular dynamics in ordered lipid systems: cholesterol reorientation in oriented lipid bilayers. *J. Am. Chem. Soc*. 112:1697–1704.
31. Mayer, C., G. Gröbner, K. Müller, K. Wiesz, and G. Kothe. 1990. Orientation-dependent deuteron spin-lattice relaxation times in bilayer membranes: characterization of overall lipid motion. *Chem. Phys. Lett*. 165:155–161.
32. Nevzorov, A. A., T. P. Trouard, and M. F. Brown. 1998. Lipid bilayers dynamics from simultaneous analysis of orientation and frequency dependence of deuterium spin-lattice and quadrupolar order relaxation. *Phys. Rev. E Stat. Phys. Plasmas Fluids Relat. Interdiscip. Topics*. 58:2259–2281.
33. Williams, G. D., J. M. Beach, S. W. Dodd, and M. F. Brown. 1985. Dependence of deuterium spin-lattice relaxation rates of multilamellar phospholipid dispersions on orientational order. *J. Am. Chem. Soc.* 107:6868–6873.
34. Brown, M. F., R. L. Thurmond, S. W. Dodd, D. Otten, and K. Beyer. 2002. Elastic deformation of membrane bilayers probed by deuterium NMR relaxation. *J. Am. Chem. Soc*. 124:8471–8484.
35. Brown, M. F., R. L. Thurmond, S. W. Dodd, D. Otten, and K. Beyer. 2001. Composite membrane deformation on mesoscopic length scale. *Phys. Rev. E*. 64:010901-1–010901-4.
36. May, S., D. Harries, and A. Ben-Shaul. 2000. Lipid demixing and protein-protein interactions in the adsorption of charged proteins on mixed membranes. *Biophys. J*. 79:1747–1760.
37. Tzlil, S., D. Murray, and A. Ben Shaul. 2008. The ''electrostatic-switch'' mechanism: Monte Carlo study of MARCKS-membrane interaction. *Biophys. J*. 95:1745–1757.
38. Koenig, B. W., L. D. Bergelson, K. Gawrisch, J. Ward, and J. A. Ferretti. 1995. Effect of the conformation of a peptide from gp41 on binding and domain formation in model membranes. *Mol. Membr. Biol*. 12:77–82.
39. Clayton, J. C., E. Hughes, and D. A. Middleton. 2005. The cytoplasmic domains of phospholamban and phospholemman associate with phospholipid membrane surfaces. *Biochemistry*. 44:17016–17026.
40. Franzin, C. M., and P. M. Macdonald. 2001. Polylysine-induced ^2H NMR-observable domains in phosphatidylserine/phosphatidylcholine lipid bilayers. *Biophys. J*. 81:3346–3362.
41. Vist, M. R., and J. H. Davis. 1990. Phase equilibria of cholesterol/dipalmitoylphosphatidylcholine mixtures: ^2H nuclear magnetic resonance and differential scanning calorimetry. *Biochemistry*. 29:451–464.
42. Demel, R. A., K. R. Bruckdorfer, and L. L. van Deenen. 1972. The effect of sterol structure on the permeability of liposomes to glucose, glycerol and Rb^+. *Biochim. Biophys. Acta*. 255:321–330.
43. Ipsen, J. H., O. G. Mouritsen, and M. Bloom. 1990. Relationships between lipid membrane area, hydrophobic thickness, and acyl-chain orientational order. The effects of cholesterol. *Biophys. J*. 57: 405–412.
44. Ohvo-Rekila, H., B. Ramstedt, P. Leppimaki, and J. P. Slotte. 2002. Cholesterol interactions with phospholipids in membranes. *Prog. Lipid Res*. 41:66–97.
45. Scheidt, H. A., D. Huster, and K. Gawrisch. 2005. Diffusion of cholesterol and its precursors in lipid membranes studied by ^1H PFG MAS NMR. *Biophys. J*. 89:2504–2512.
46. McIntosh, T. J. 2007. X-ray diffraction to determine the thickness of raft and nonraft bilayers. *Methods Mol. Biol.* 398:221–230.
47. Veatch, S. L., O. Soubias, S. L. Keller, and K. Gawrisch. 2007. Critical fluctuations in domain-forming lipid mixtures. *Proc. Natl. Acad. Sci. USA*. 104:17650–17655.

48. Hsueh, Y. W., M. T. Chen, P. J. Patty, C. Code, J. Cheng, et al. 2007. Ergosterol in POPC membranes: physical properties and comparison with structurally similar sterols. *Biophys. J.* 92:1606–1615.

49. Bartels, T., R. S. Lankalapalli, R. Bittman, K. Beyer, and M. F. Brown. 2008. Raftlike mixtures of sphingomyelin and cholesterol investigated by solid-state ^{2}H NMR spectroscopy. *J. Am. Chem. Soc.* 130:14521–14532.

50. Bunge, A., P. Muller, M. Stockl, A. Herrmann, and D. Huster. 2008. Characterization of the ternary mixture of sphingomyelin, POPC, and cholesterol: support for an inhomogeneous lipid distribution at high temperatures. *Biophys. J.* 94:2680–2690.

51. Soni, S. P., D. S. LoCascio, Y. Liu, J. A. Williams, R. Bittman, et al. 2008. Docosahexaenoic acid enhances segregation of lipids between: ^{2}H-NMR study. *Biophys. J.* 95:203–214.

52. Pechlivanis, M., and J. Kuhlmann. 2006. Hydrophobic modifications of Ras proteins by isoprenoid groups and fatty acids—more than just membrane anchoring. *Biochim. Biophys. Acta.* 1764:1914–1931.

53. Brunsveld, L., J. Kuhlmann, K. Alexandrov, A. Wittinghofer, R. S. Goody, et al. 2006. Lipidated ras and rab peptides and proteins—synthesis, structure, and function. *Angew. Chem. Int. Ed. Engl.* 45: 6622–6646.

54. Silvius, J. R. 2002. Mechanisms of Ras protein targeting in mammalian cells. *J. Membr. Biol.* 190:83–92.

55. Gorfe, A. A., R. Pellarin, and A. Caflisch. 2004. Membrane localization and flexibility of a lipidated ras peptide studied by molecular dynamics simulations. *J. Am. Chem. Soc.* 126:15277–15286.

56. Gorfe, A. A., M. Hanzal-Bayer, D. Abankwa, J. F. Hancock, and J. A. McCammon. 2007. Structure and dynamics of the full-length lipid-modified H-Ras protein in a 1,2-dimyristoylglycero-3-phosphocholine bilayer. *J. Med. Chem.* 50:674–684.

57. Feller, S. E., K. Gawrisch, and A. D. MacKerell, Jr. 2002. Polyunsaturated fatty acids in lipid bilayers: intrinsic and environmental contributions to their unique physical properties. *J. Am. Chem. Soc.* 124: 318–326.

58. Huster, D., K. Arnold, and K. Gawrisch. 1998. Influence of docosahexaenoic acid and cholesterol on lateral lipid organization in phospholipid mixtures. *Biochemistry.* 37:17299–17308.

59. McLaughlin, S., and D. Murray. 2005. Plasma membrane phosphoinositide organization by protein electrostatics. *Nature.* 438:605–611.

60. Gonzalez-Horta, A., D. Andreu, M. R. Morrow, and J. Perez-Gil. 2008. Effects of palmitoylation on dynamics and phospholipid-bilayer-perturbing properties of the N-terminal segment of pulmonary surfactant protein SP-C as shown by ^{2}H-NMR. *Biophys. J.* 95:2308–2317.

61. Liang, X., A. Nazarian, H. Erdjument-Bromage, W. Bornmann, P. Tempst, et al. 2001. Heterogeneous fatty acylation of Src family kinases with polyunsaturated fatty acids regulates raft localization and signal transduction. *J. Biol. Chem.* 276:30987–30994.